Heat Shielding for Venus Entry Probes

DAVID L. PETERSON*
NASA Ames Research Center, Moffett Field, Calif.
AND
WILLIAM E. NICOLET†
Acurex Corp., Mountain View, Calif.

The initial exploration of Venus by the proposed Pioneer Venus will be conducted as a multiple entry mission. A major probe will enter the planet, accompanied by three miniprobes that may enter at steep to shallow angles. The heating environment will present sizable convective and radiative heating levels as well as significant shear forces to the heat shields. Two contrasted approaches to ablative thermal protection are presented—a typical carbonaceous charring ablator and a dielectric reflective ablator. The primary variance in the two techniques lies in their optical properties: the charring material is highly absorptive to the gas-cap radiation and the dielectric is highly reflective. The interesting observation in this study is that mass loss is not the controlling variable in heat-shield sizing. A heat-soak problem determines the carbon phenolic sizing. For Teflon, the material thickness required to accomplish reflection is the sizing factor. The total heat-shield weight required to handle either steep or shallow entry is computed to be 13% less for a Teflon shield (if at least 3.2 mm required for reflection) than for a charring ablator shield. If an efficient reflective backing is used with Teflon, the thickness can be reduced 1.0 mm and the computed weight is 31% less for Teflon than for the charring ablator. Such weight reductions may significantly increase the science payload weight of the miniprobes.

Introduction

THE introduction of heat-shield materials that can reflect incident radiation from the gas cap of entry vehicles has broadened the technology available for the design of thermal protection systems subjected to radiative heating environments.[1] One such mission is the proposed multiple entry probe of Pioneer Venus.[2] One main probe and three miniprobes will simultaneously enter the planet and be subject to both convective and radiative heating loads on the order of several kilowatts per square centimeter. The traditional approach, which appears capable of withstanding such environments, is the well-known carbonaceous charring ablators. The environment is complicated, however, by considerable shear forces in a regime unproven for most charring materials. High-density carbon phenolic (proposed in the Phase B final study of Pioneer Venus[2]) was examined in this study as a characteristic charring ablator with good char integrity.[3] Of course, black materials absorb all the incident radiation and then reradiate a sizable portion from the high-temperature carbon char. The alternative approach is a diffusely reflecting dielectric material.[1] A substantial fraction of the radiative flux can be rejected by a thin Teflon (TFE) shield backed by a highly reflective backface structure. The benefit in heat-shield weight by tradeoffs in reflection vs absorption/reradiation may be marginal for the modest entry environments of the Pioneer Venus probe. Indeed, other mechanisms or features may be more significant in selecting and sizing candidate heat-shield materials. The following discussion will examine the heating environment and the response of the aforementioned materials to this environment which leads to criteria for sizing the heat shield. A preliminary experimental study to optimize the reflective approach is also presented as motivated by the theoretical analysis.

Analysis of the Environment

The nature of the response of a reflective dielectric heat shield to a convective/radiative environment dictates a different approach to probe design, namely, a blunter shape to reduce convection and enhance radiation, thereby exploiting the reflective virtues of the dielectric. Two probe shapes were therefore considered, a modified Apollo shape (blunt) and a spherically tipped 60° half-angle cone (Fig. 1). Both shapes were considered to be candidates for the small probe mission, whereas only the blunted cone was considered for the large probe mission. Trajectory data are presented in Figs. 2a–2c for entry angles and ballistic coefficients of $-37°$ and 78 kg/m^2 (large probe) and $-24°$ and $-75°$ and 136 kg/m^2 (small probes), which are typical for the Venus mission.[2] Calculations were performed with a simplified model assuming a point mass in an exponential atmosphere.[4]

The inviscid, adiabatic flowfield events about the body were obtained from correlations. Kaattari's approach[5] was used to obtain the shock shape and standoff distances. Then (for the modified Apollo shape), the Rankine-Hugoniot equations were solved at the specified shock angles to yield the shock-layer

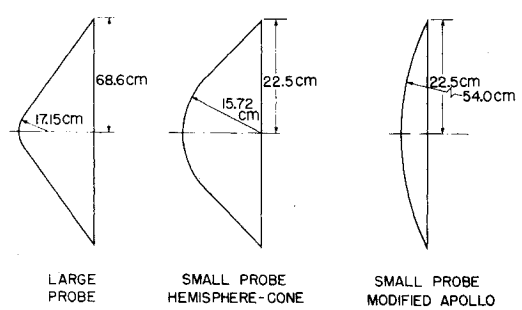

Fig. 1 Probe shapes.

Presented as Paper 73-712 at the AIAA 8th Thermophysics Conference, Palm Springs, Calif., July 16–18, 1973; submitted August 8, 1973; revision received January 10, 1974. The authors wish to acknowledge the contributions in the analysis by K. Suchsland, C. Derbidge, C. Moyer, and M. Wool of Acurex-Aerotherm and O. Zappa of AVCO-Wilmington; and in the experiments by J. Hagen of NASA Ames.

Index categories: Entry Vehicles and Landers; Material Ablation; Radiation and Radiative Heat Transfer.

* Research Scientist.

† Manager, Aerochemistry Department, Aerotherm Division. Member AIAA.

Table 1 Composition and properties of carbon phenolic (45° layup)

Nominal density, g/cm³	Nominal resin fraction	Resin residual	Assumed resin elemental formula	Reinf. elemental formula	Temperature, °K	Virgin material: Spec. heat, cal/gm-°K	Virgin material: Thermal conduct., cal/cm-sec-°K	Virgin material: Emissivity	Char: Spec. heat, cal/gm-°K	Char: Thermal conduct., cal/cm-sec-°K	Char: Emissivity
1.432	0.345	0.40	C_6H_6O	C	295	0.210	30.4×10^{-4}	0.9	0.210	34.5×10^{-4}	0.9
					445	0.360	32.1	0.9	...	...	0.9
					555	0.360	32.1	0.9	0.430	43.2	0.9
					644	0.360	34.5	0.9	...	...	0.9
					830	0.472	34.5	0.9	0.472	56.6	0.9
					1110	0.484	34.5	0.9	0.484	74.4	0.9
					1670	0.493	34.5	0.9	0.493	128.0	0.9
					2220	0.498	34.5	0.9	0.498	205.3	0.9
					2780	0.500	34.5	0.9	0.500	296.0	0.9
					3330	0.500	34.5	0.9	0.500	403.2	0.9

pressures, an approach nearly equivalent to the usual modified Newtonian approach. The pressure distributions about the blunted cone were obtained directly from experimental data. The boundary-layer-edge velocities were obtained by calculating an isentropic expansion to the local pressure.

In calculating the cold-wall, convective heating environment, the adiabatic, inviscid edge conditions were used with an integral boundary-layer procedure (the ARGEIBL program‡[6]) to obtain the required fluxes. The use of the adiabatic edge conditions is justified by earlier calculations of Hoshizaki and Wilson[8] and others[9] who found that radiation losses in the shock layer have small effects on convective heating. Both laminar and turbulent heating events were considered with transition required to occur at $Re_\theta = 200$.§ Under this constraint, turbulent heating was found to dominate in the skirt region for nearly all the cases considered.

In calculating the radiation heating environment, the thermodynamic conditions were obtained at the shock-wave point directly opposite the body point of interest and assumed to be uniform across the inviscid part of the shock layer. These conditions were used with a detailed radiation transport procedure (the RADICAL program¶[10,11]) that calculated the fluxes incident from a uniform, plane-parallel slab tangent to the body at the point of interest. The use of the plane-parallel slab approximation should yield predicted fluxes that are about 15% high in the stagnation region of the blunted cone, are also high (but less so) for the stagnation region of the Apollo shape, and are in very good agreement in the skirt region of the blunted cone (see Ref. 14). These fluxes were subsequently corrected for radiation cooling and (cold wall) boundary-layer absorption with a correlation based on the data of Page and Woodward[15] calculated for an atmosphere (90% CO_2/10% N_2) close to that assumed here.

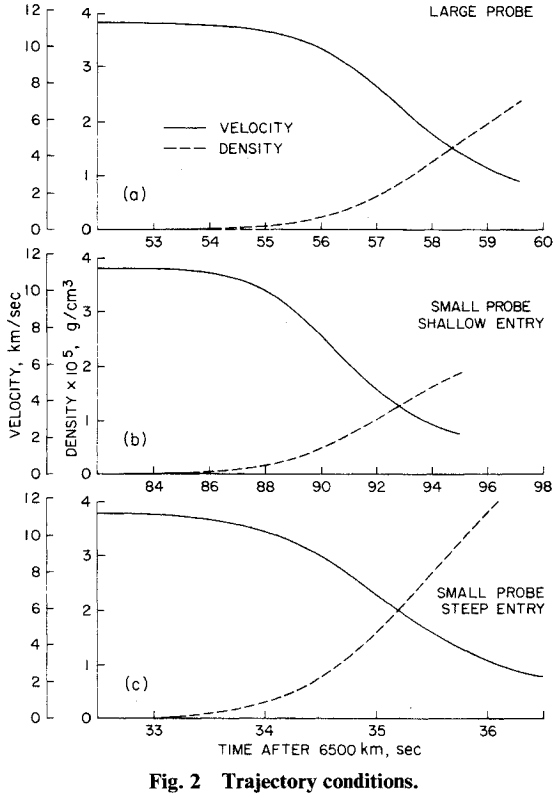

Fig. 2 Trajectory conditions.

Analysis of the Heat Shield

The responses of semi-infinite slabs of the candidate Teflon and carbon phenolic heat-shield materials were evaluated at the

Table 2 Carbon phenolic decomposition kinetic constants[a]

Reaction i	Pre-exponential factor B_i, sec^{-1}	Activation energy factor Ea/R, °K	Density factor exponent ψ	Initial density ρ_{o_i}, g/cm³	Residual density ρ_{r_i}, g/cm³
A	1.4×10^4	8560	3	0.324	0
B	4.48×10^9	20440	3	0.973	0.519

[a] In characterizing resin decomposition, two parallel, kinetically controlled reactions are assumed having the form

$$\frac{\partial \rho_i}{\partial \theta} = B_i e^{-E_{a_i}/RT} \rho_{o_i} \left(\frac{\rho_i - \rho_{r_i}}{\rho_{o_i}} \right)^{\psi}$$

where ρ_i is the density of the ith component.

‡ The ARGEIBL program uses the integral approach to solve the nonsimilar boundary-layer energy equation. Real gas effects were considered explicitly through the use of a tabulated Mollier diagram generated for the assumed 95% CO_2/5% N_2 Venus atmosphere. Transport properties were obtained from the study of Thomas[7] for pure CO_2.

§ Since the boundary-layer program integrates only the energy equation, only the energy thickness is available (not θ). Therefore, transition is actually caused to occur when the energy thickness Reynolds number exceeds the transition Reynolds number. However, differences in the momentum- and energy-based Reynolds numbers are expected to be insignificant compared to uncertainties in the transition Reynolds numbers.

¶ The RADICAL program performs a moderately detailed integration of the radiation transport equations. For the CO_2-N_2 atmosphere of interest, it considers photoionization, free-free, photodissociation, photodetachment, 12 molecular band systems, and approximately 100 atomic and ionic lines. Typically, the fluxes calculated are slightly above those of Stickford[12] and slightly below those of Avilova et al.[13]

Table 3 Composition and properties of Teflon

Nominal density, g/cm³	Assumed elemental formula	Temperature, °K	Specific heat, cal/g-°K	Thermal conductivity, cal/cm-sec-°K	Emissivity
2.18	C_2F_4	295	0.25	9.97×10^{-4}	0
		550	0.25	9.97	0
		830	0.25	9.97	0
		1100	0.25	9.97	0

Table 4 Teflon decomposition kinetic constants[a]

Pre-exponential factor β_2, cm/sec	Activation energy factor β_4, °K
2.86×10^{20}	4.06×10^4

[a] The Teflon kinetics are assumed to be controlled by a reaction of the form

$$\dot{s} = \beta_2 \exp(-\beta_4/T)$$

where $\dot{s}$ is the recession rate.

environmental conditions corresponding to the $R/R_{max} = 0.7$ point on each of the bodies. The material properties used are presented (in part) in Tables 1–4, where the properties are considered typical for both materials and the carbon phenolic properties assume a 45° layup. A surface emissivity of 0.9 was assumed for the carbon phenolic char. For the Teflon, the in-depth refractive properties were approximated by assuming unit reflectivity. This assumption is supported by experimental tests of Teflon in a combined heating environment.** By this mechanism, the incident radiation flux is caused to disappear from the system so the Teflon results should be viewed as optimistic.

The surface events of interest were represented by a film coefficient model that accounts for the surface thermochemical events in detail and also accounts for the effects of blowing on the reduction of the incident convective flux but neglects the effects in reducing the incident radiation flux.††

The convective blowing correction is obtained from a correlation of the form

$$C_H/C_{H_o} = 2\lambda B_o'/\exp(2\lambda B_o') - 1$$

where λ was taken to be 0.4 for turbulent flow and 0.6 for laminar flow.‡‡ For carbon phenolic, the surface thermochemical events assumed equilibrium between the edge gas, pyrolysis gas, and char, and the candidate species were taken from the JANAF[18] tables without *a priori* preference. For Teflon, the kinetically controlled surface decomposition model of Steg and Lew[19] was used along with the quasi-equilibrium energy statement of Greenberg et al[20] which assumes that CF_3 and CF_4 will not have time to form and, consequently, are not included among the candidate species.

The in-depth thermal analysis was performed using a charring material ablation procedure (the CMA program[21]) that considers decomposition in depth, heat conduction with temperature-dependent properties, heat removal by the pyrolysis gases (assumed to be in equilibrium with the char), coupling to the thermochemical and flowfield events at the surface, and the effects of the moving boundary. The results will be discussed in the next section.

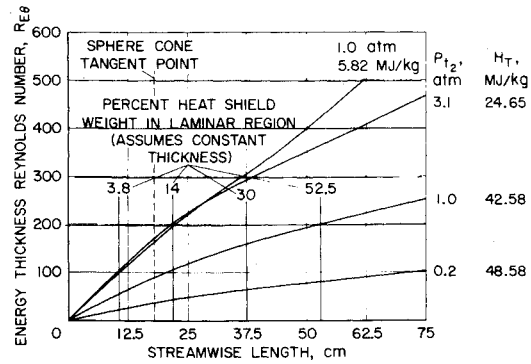

Fig. 3 Transition Reynolds number and streamwise location for various pressures and enthalpies.

Results of the Analysis

The first set of calculations was obtained to assess the sensitivity of the over-all heat-shield environment to the selection of the transition Reynolds number (Re_{θ_t}). As shown in Fig. 3, roughly half the heat-shield weight will be subject to turbulent flow for at least part of the trajectory provided $Re_{\theta_t} < 350$. For a more typical value of $Re_{\theta_t} \sim 200$, about 70% of the heat-shield weight will be subject to turbulent flow (nearly) throughout the entire hypersonic heating pulse. Consequently, it appears that the heat shield will have to be designed to withstand turbulent flow for any reasonable selection of Re_{θ_t}. The potential weight penalties are serious since the maximum convective heating (and total heating) will occur near the skirt where the greatest fraction of the heat-shield surface is exposed.

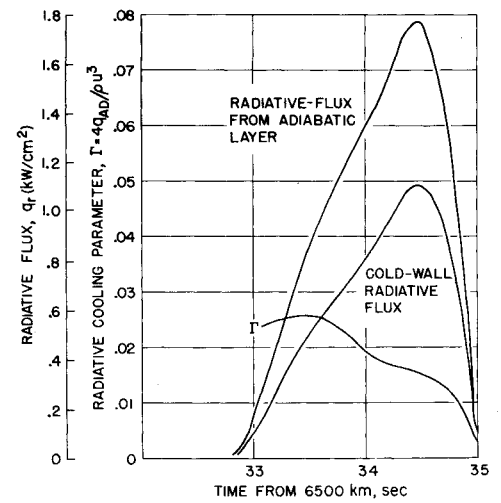

Fig. 4 Typical radiative heating profiles for small probe, steep entry.

** These tests indicate that, for the radiation spectrum of the facility (see Ref. 23) used, the surface recedes as if the radiative flux is entirely reflected (see Ref. 1 or 16). Teflon, in fact, has a very low absorption coefficient and reacts weakly to the radiative heating.[17] A semi-infinite slab of Teflon will approach unit reflectivity between 0.25 and 2.0 μ wavelength and begins to absorb near the surface in the ultraviolet. Reference 1 shows that 3.2 mm of Teflon can reflect 75% of the radiation in this band and, indeed, reflects nearly all the radiation at longer wavelengths when backed by a highly reflective surface (silver).

†† The radiation fluxes were allowed to pass unattenuated through the ablation products. This should be viewed as an assumption, as correlations of the blowing reduction are not available for Venus entry. However, if one uses existing correlations for entry into other planetary atmospheres (i.e., Jupiter), one would predict little attenuation.

‡‡ Neither rough wall effects nor mechanical removal are considered as part of the surface model. The effect on Teflon ablation is probably very small because of its low surface temperature, relatively smooth surface features during the ablation, and (typically) high blowing rates. These effects should be more important for carbon phenolic than for Teflon, but should still be small because 1) little material will be removed from the surface (hence it will remain relatively smooth); 2) carbon phenolic forms a tough char that tends to retain its integrity and resist mechanical removal[3]; and 3) heat soak events (of dominant importance for heat shields of this material) are only moderately sensitive to the details of the incident flux.

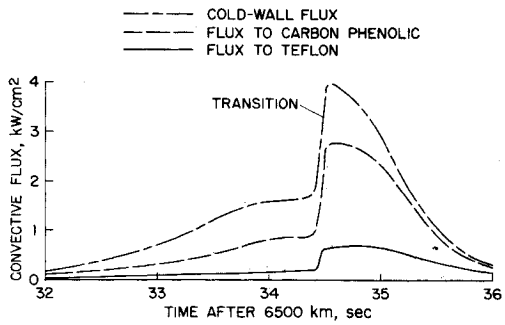

Fig. 5 Typical convective heating pulses for small probe steep entry.

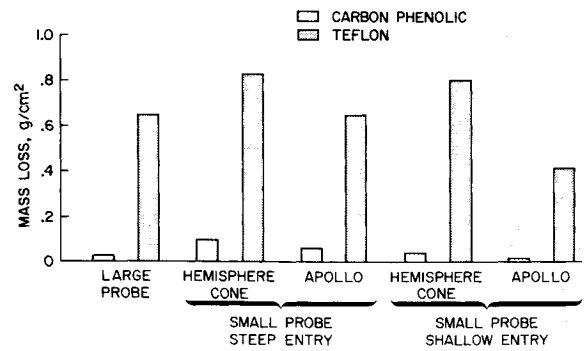

Fig. 7 Total mass loss for carbon phenolic and Teflon.

The radiative and convective fluxes are shown in Figs. 4 and 5 for the small probe during steep entry. The radiative cooling and (unblown) boundary-layer absorption combine to reduce the incident radiative flux to about 60–65% of the isothermal value, irrespective of the probe shape, entry angle, or heat-shield material. In contrast, the convective flux to the wall depends strongly on the heat-shield material, with the fluxes to the Teflon surface being far lower (factor of 5 to 10) than the cold-wall fluxes and substantially lower than those to the carbon phenolic wall. The convective flux is also strongly influenced by transition that occurs near peak heating conditions for the case shown. If transition were to occur earlier (e.g., 33.5 sec), the time-integrated, cold-wall flux would be increased by about 30% (Fig. 6).

The time-integrated heating loads are shown in Fig. 6. As shown, the modified Apollo shape receives about 20–30% less convective loads than the small probe hemisphere-cone and about a factor of 2 greater radiation load. Thus, the total heating load (convective only) to a Teflon body is reduced by 20–30% by using the modified Apollo shape (as expected), whereas the total load on a carbon phenolic body (convective plus radiation) is nearly independent of the body shape. In all cases, the total heating load to a Teflon body is a factor of 5 to 10 less than the total loads on a carbon phenolic body.

The total ablative mass losses, typical temperature distributions, and heat-shield sizing requirements are shown in Figs. 7–10. In Fig. 7, the total mass loss from carbon phenolic is shown to be an order of magnitude less than that lost from Teflon. However, the heat-shield sizing is not determined by the mass loss for either material. Typical in-depth temperature distributions are shown in Figs. 8 and 9. Teflon remains much cooler in depth during entry, an important consideration for the small probes where the heat shields will not be jettisoned. For carbon phenolic, the heat soak problem is severe. §§ The heat shield was sized by requiring that the bondline temperature remain less than 1000°R. For Teflon, the problem of shielding the backup structure from the incident radiation flux is critical. The heat-shield size was determined by requiring that a minimum thickness of 3.2 mm be present throughout the radiation pulse. When combined with a highly reflective backface (e.g., a silver-deposit coating on the backup structure), this thickness will achieve nearly unit reflectance for the longer visible and infrared wavelengths that can be partially transmitted by the Teflon.[1]

The heat-shield size requirements are presented in Fig. 10. Over-all, the Apollo shape/Teflon combination appears to offer

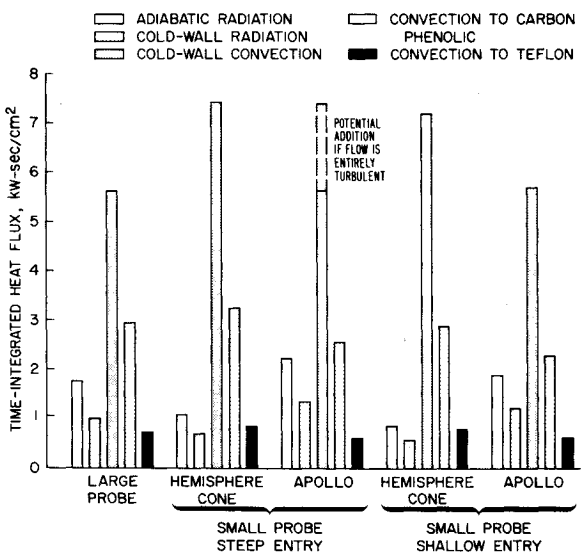

Fig. 6 Time-integrated heat fluxes for various probe shapes, sizes, and entry angles.

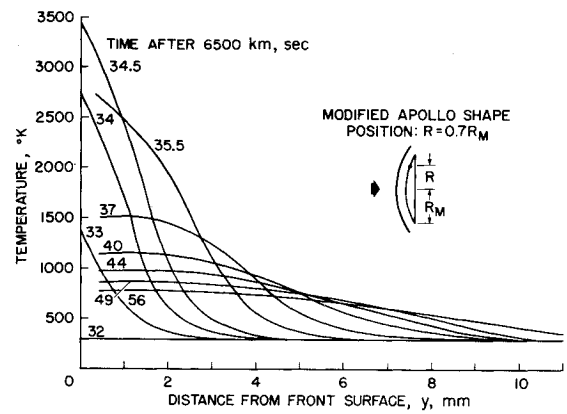

Fig. 8 In-depth temperature distribution for carbon phenolic for small probe, steep entry.

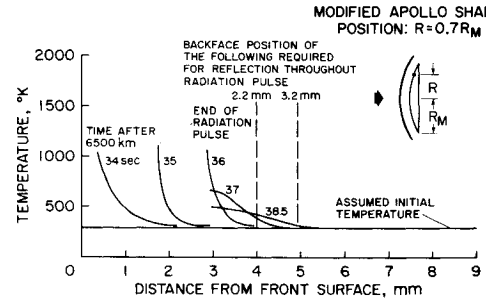

Fig. 9 In-depth temperature distributions for a Teflon heat shield for small probe, steep entry.

§§ This alleviates many of the uncertainties associated with roughness-augmented convection and mechanical removal because the heat soak is primarily a function of surface temperature and is only moderately sensitive to the incident flux.

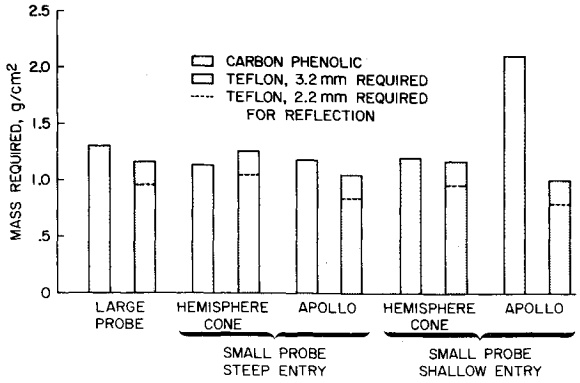

Fig. 10 Heat-shield sizing requirements.

slightly lower weight than either the hemisphere-cone/Teflon combination or the hemisphere-cone/carbon phenolic combination, although the differences are small. The weight of the Teflon probes could be significantly reduced if the minimum thickness required for complete reflection could be reduced from 3.2 to 2.2 mm (for example), as shown by the dotted lines in Fig. 10. The identification of the reflective properties of the Teflon heat-shield structure as a dominant heat-shield sizing requirement was unexpected and is viewed as one of the more significant results of the analysis. This observation motivated the experimental study (described in the following sections) to optimize the reflective properties of the heat-shield structure.

Experimental Study

Reducing the thickness of the Teflon shield is desirable from a point of view of saving weight but requires that at least two conditions be met. First, the over-all reflection of radiation must be maintained and second, protection from the convective heating must be preserved. Regarding the second condition, little or no heat soak problem exists for Teflon as shown in Fig. 9. Reducing the thickness by 20% incurs only a slight increase in the effects of conduction. The first condition stipulates that the thinner Teflon thickness does not result in such a degraded reflective performance that a serious hazard is created at the backface due to transmitted radiation. The Teflon itself accomplishes a major portion of the reflectance as shown in Fig. 11. As the reflectance is only a weak function of thickness in this thickness range and wavelength spectrum, the slight overall loss of reflection becomes a modest increase in transmittance to the backface. The transmitted energy is roughly 20–30% in this spectrum and would be entirely absorbed if the backface were black. However, the backface can be highly reflective itself and then the over-all reflectance is not only maintained but significantly improved.

Several combinations of Teflon and a reflective backface were examined experimentally to evaluate this potential reflection improvement. A diffuse white coating (Kodak white reflective paint, $BaSO_4$,[22] commonly used in integrating spheres) and two

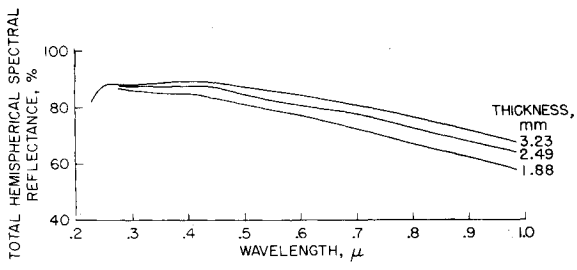

Fig. 11 Reflectance of several thicknesses of Teflon backed by a black surface.

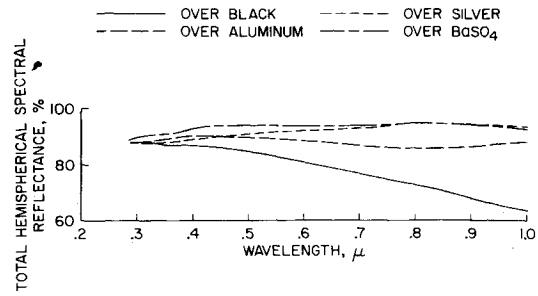

Fig. 12 Reflectance of 2.49 mm of Teflon backed by several reflective surfaces.

specular metallic coatings (vapor-deposited aluminum and silver with a silicon oxide overcoat) were examined. The reflectance of each coating behind 2.49 mm of Teflon is shown in Fig. 12 and compared to a black backface. In this virgin state, the $BaSO_4$ provides the best over-all performance. Most of the improvement occurs at the longer wavelengths where Teflon effectively transmits. At the ultraviolet end, Teflon itself accomplishes nearly all the reflection; the backface hardly sees the shorter wavelengths. The nonreflected radiation is reduced to less than 10% of the incident flux, and is absorbed by either the Teflon or the backface.

Whether these coatings could be preserved in the presence of realistic flight heating levels is a matter of concern. For an incident flux of 1.0 kw/cm², 0.2 to 0.3 kw/cm² would be present at the backface when the Teflon is about 2 to 3 mm thick. A test model was configured to evaluate the sustained integrity of these coatings in a realistic combined heating test environment.[23] Transient hemispherical slug calorimeters (Fig. 13, inset) covered by a Teflon shroud of constant thickness were exposed to combined convective and radiative heating. The 1.5-cm-diam calorimeters were coated with the reflective coatings, with a blackened one used as control. The spectrum of imposed radiation from the argon radiation source is also shown in Fig. 13. The model environment consisted of 1100 w/cm² convective heating in air at 0.25 atm stagnation pressure and a radiative heating rate of 1500–1600 w/cm². The backface flux seen by the calorimeters was measured by the black-coated model to be about 400 w/cm². The diffuse coating, $BaSO_4$, discolored distinctly and the aluminum surface darkened during the test, leading in both cases to a loss of reflectance and increased absorption of the backface flux. The reflectivity of these coatings dropped to about 70–75%, creating an absorption of flux of about 50% in contrast to the expected value of less than 10%. The silver reflective properties remain intact, however, absorbing about 9% of the initial incident flux. This value agrees well with the expected values, representing about 30% of the backface flux. The potential for further reducing backface absorption as well as ensuring a stable coating

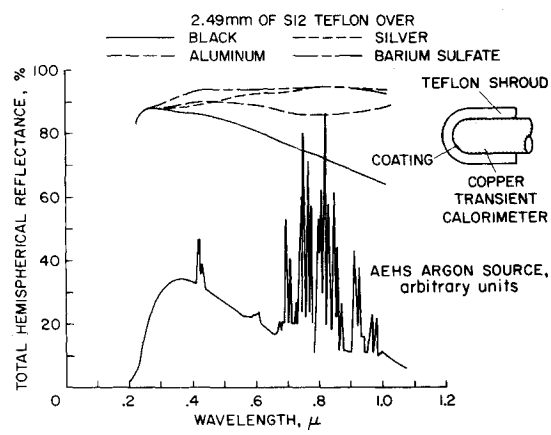

Fig. 13 Reflectance of 2.5-mm Teflon over several reflective surfaces and the spectrum of the argon radiation source.

appears reasonable. The interesting fact is that a reduction in thickness of Teflon (say from 3.2 to 2.5 mm) which increases the transmittance 4–6%, leads to less than a 1% increase in absorption of the initial energy for an 85% reflective coating. Thus, it can be reasonably expected that the Teflon thickness can be minimized without jeopardizing the performance and safety of the heat shield. The additional reduction in weight committed to a Teflon shield for each case is shown by the dotted lines in Fig. 10. These lines indicate that if 1.0 mm less of Teflon were required then the over-all weight of the Teflon shield could be diminished by roughly 20%. Thus, 2.2 mm rather than 3.2 mm of Teflon would be maintained to preserve the reflectance of the heat shield throughout the radiation pulse.

Summary and Conclusion

A comparative analysis was conducted for two concepts: carbon phenolic, a charring ablator, and Teflon, a reflective dielectric ablator. The study reveals that mass loss is not a prime factor in sizing the heat shield in either case. Carbon phenolic loses very little mass, responding to the entry environment as a heat sink with its sizing controlled by the bond-line temperature. Teflon soaks little or no energy but loses significant mass. It is sized by the requirement that sufficient material be present to achieve reflection throughout the radiation pulse. The thickness chosen for comparison was 3.2 mm of Teflon (remaining at the conclusion of the radiation pulse), which by itself accomplishes about 75% reflection of the radiation.

Despite the reflection requirement and rapid ablation, a Teflon shield still shows a slight weight advantage over a charring ablator shield. For economy on the miniprobes, only one design can be considered for all entries. With this constraint, the total heat-shield weight required to handle either a steep entry or a shallow entry is computed to be 13% less for a Teflon shield (Apollo shape/steep entry) than for a carbon phenolic heat shield (hemisphere cone/shallow entry). For the large probe, Teflon shows an 11% advantage. The effect of probe shape in the analysis has shown that the advantages of material and shape combinations are not dramatic except in the case of the carbon phenolic/Apollo shape, which is markedly inferior to all cases.

The experimental study has shown that Teflon, backed by a good reflective surface, can withstand the heating environment with a reduced thickness required for reflection. The requirement of 3.2 mm could be reduced as much as 1.0 mm without seriously altering the reflective performance. This feature can be viewed in two ways. One viewpoint is the assurance that the payload fraction of the probes will not be encroached upon by weight fluctuations in the design of the heat shield. The other is the 1.0 mm reduction in required thickness be considered a potential savings of heat-shield weight. The total heat-shield weight for a Teflon (2.2 mm required) shielded reflector is 31% less than the charring ablator shield for the miniprobes and 27.5% less for the large probe. Such weight reductions may offer significant increases in the science payload weight of either probe, but especially the miniprobe.

References

[1] Nachtsheim, P. R., Peterson, D. L., and Howe, J. T., "Reflecting Ablative Heat Shields for Radiative Environments," AAS Paper 71-47, Seattle, Wash., 1971.

[2] Dorfman, S. D., "System Design of the Pioneer Venus Spacecraft," Vol. 5, Probe Vehicle Studies, Final Report, NASA Contract NAS2-7249, Hughes Aircraft Co., Culver City, Calif.; also CR 114591, July 1973, NASA.

[3] Moyer, C. B., Suchsland, K. E., and Bartlett, E. P., "Fundamental Ablative Mechanisms of Reinforced Aromatic/Heterocyclic Resin Composites," Rept. 72-55, June 1972, Aerotherm Div., Acurex Corp., Mountain View, Calif.

[4] Allen, H. J. and Eggers, A. J., "A Study of the Motion and Aerodynamic Heating of Ballistic Missiles Entering the Earth's Atmosphere at High Supersonic Speed," Rept. 1381, 1958, NACA.

[5] Kaattari, George E., "Shock Envelopes of Blunt Bodies at Large Angles of Attack," TN D-1980, 1963, NASA.

[6] McCuen, P. A., Schaefer, J. W., Lundberg, R. E., and Kendall, R. M., "A Study of Solid-Propellant Rocket Motor Exposed Materials Behavior," Final Rept., Contract AF. Or(611)09073, Feb. 1965, Vidya Div., Itek Corp., Palo Alto, Calif.; also "User's Manual for the Aerotherm Real Gas Energy Integral Boundary Layer Program," Rept. 69-UM-6911, Nov. 1969, Aerotherm Div., Acurex Corp., Mountain View, Calif.

[7] Thomas, M., "The High Temperature Transport Properties of Carbon Dioxide," Rept. SM-37790, July 1960, Douglas Aircraft Co., Inc., Missiles and Space Systems Engineering, Santa Monica, Calif.

[8] Hoshizaki, H. and Wilson, K. H., "Convective and Radiative Heat Transfer During Superorbital Entry," *AIAA Journal*, Vol. 5, No. 1, Jan. 1967, pp. 25–35.

[9] Chou, Y. S. and Blake, L. H., "Energy-Momentum Coupling in Radiating Shock Layers About a Blunt Body," *AIAA Journal*, Vol. 8, No. 9, Sept. 1970, pp. 1680–1686.

[10] Nicolet, W. E., "Advanced Methods for Calculating Radiation Transport in Ablation Product Contaminated Boundary Layers," CR-1656, Sept. 1970, NASA.

[11] Nicolet, W. E., "User's Manual for the Generalized Radiation Transfer Code (RAD/EQUIL)," Rept. UM-69-9, Oct. 1969, Aerotherm Corp., Mountain View, Calif.

[12] Stickford, G. H., Jr., "Total Radiative Intensity Calculations for 100 Percent CO_2 and 90 Percent CO_2—10 Percent N_2," *Journal of Quantitative Spectroscopy and Radiative Transfer*, Vol. 10, No. 4, April 1970, pp. 249–279.

[13] Avilova, I. V., Biberman, L. M., Vorobjev, V. S., Zamalin, V. M., Kobzev, G. A., Lagar'kov, A. N., Mnatsakanian, A. Ch., and Norman, G. E., "Optical Properties of Heated Air—II: Integral Characteristics 4000–20000°K," *Journal of Quantitative Spectroscopy and Radiative Transfer*, Vol. 9, No. 1, Jan. 1969, pp. 113–122.

[14] Wilson, K. H., "Evaluation of One-Dimensional Approximations for Radiative Transport in Blunt Body Shock Layers," CR-1990, March 1972, NASA.

[15] Page, W. A. and Woodward, H. T., "Radiative and Convective Heating During Venus Entry," *AIAA Journal*, Vol. 10, No. 10, Oct. 1972, p. 1379.

[16] Peterson, D. L., Nachtsheim, P. R., and Howe, J. T., "Reflecting Ablating Heat Shields for Planetary Entry," *AIAA Journal*, Vol. 10, No. 11, Nov. 1972, pp. 1499–1505.

[17] Howe, J. R., Green, M. J., and Weston, K. C., "Thermal Shielding by Subliming Volume Reflectors in Convective and Intense Radiative Environments," *AIAA Journal*, Vol. 11, No. 7, July 1973, pp. 989–994.

[18] Stull, D. R. and Prophet, H., JANAF Thermochemical Tables, 2nd Ed., National Standard Reference Data Service, National Bureau of Standards (U.S.), 37, June 1971.

[19] Steg, L. and Lew H., "Hypersonic Ablation" in *The High Temperature Aspects of Hypersonic Flow*, edited by W. C. Nelson, The Macmillan Co., New York, 1964.

[20] Greenberg, R. A., Kemp, N. H., and Wray, K. L., "Structure of the Laminar Ablating Air-Teflon Boundary Layer," Research Rept. 301, Nov. 1968, AVCO-Everett Research Lab., AVCO Corp., Everett, Mass.

[21] Moyer, C. B. and Rindal, R. A., "An Analysis of the Coupled Chemically Reacting Boundary Layer and Charring Ablator," Rept. 66-7, Pt. II, March 1967, Aerotherm Div., Itek Corp., Palo Alto, Calif.

[22] "Eastman White Reflectance Paint," Publication JJ-32, July 1969, Eastman Organic Chemicals, Eastman Kodak Co., Rochester, N.Y.

[23] Peterson, D. L., Gowen, F. E., and Richardson, C. L., "Design and Performance of a Combined Radiative Convective Heating Facility," AIAA Paper 71-255, Albuquerque, N. Mex., 1971.